4.5 Recommendations

For the countermeasure of safer masonry building due to earthquake, much more improved device is indispensable especially on the seismic strength against out-of-plane falling down of brick masonry wall system.

In order to start such device development, following items will be effective;

a) to strengthen more the rotation resistance of foundation system.

b) As long as masonry structure is low rise building, in-plane shear strength of masonry wall may be enough to such level of earthquake as occurred as this time. However the out-of-plane bending resistance is very small. It is required some reinforcement or prestressing using reinforcing bars, wires and bamboos, should be installed in masonry walls with enough encourage to concrete foundation systems. If we use bamboo as reinforcement, which is available in Sikka Prefecture, it's Young's modulus and tensile strength are respectively $1.25 - 1.55 \times 105$ kg/cm^2 and $1700 - 2400$ kg/cm^2. So, bamboo can be much effective for strengthening wall system by intelligent device of construction. Such detailed construction manual for local people should be based on the test results which shall be planned and conducted in Research Institute of Human Settlements, Ministry of Public Works, Bandung.

Photo 4.1 Masonry Building in Ende Airport, No Damage

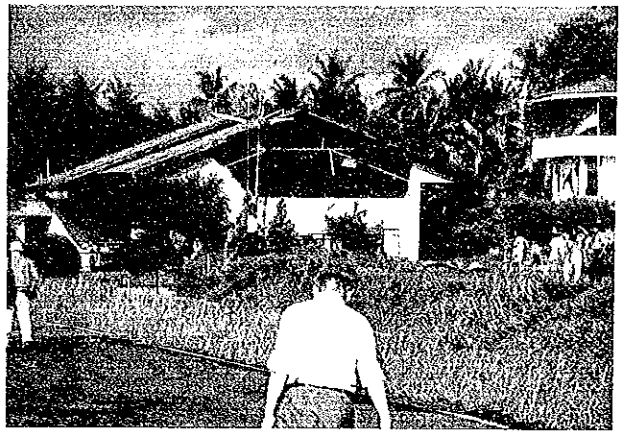

Photo 4.2 Masonry Building in Ende Airport, Falling Down of Side Upper Wall

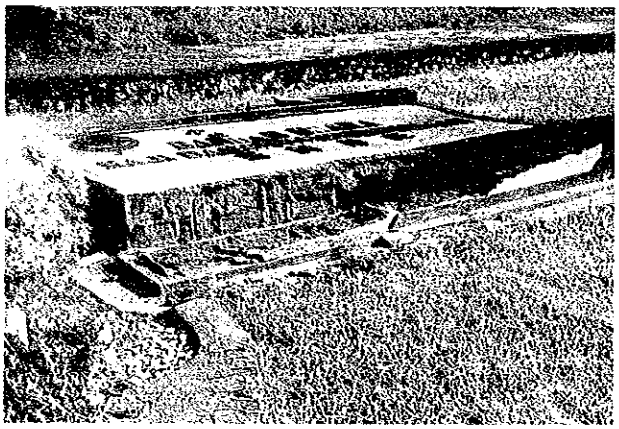

Photo 4.3 Airport Name Wall Panel, Falling Down, No Reinforcing

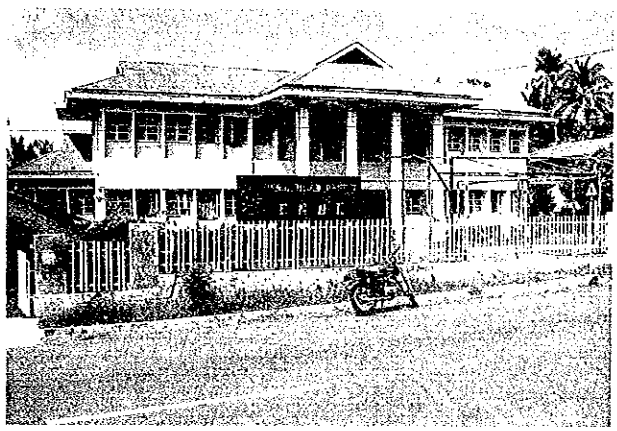

Photo 4.4 Ende City Office, Severe Damage, Remaining Story Drift 10 cm

Photo 4.5 Ende City Office, Close Up

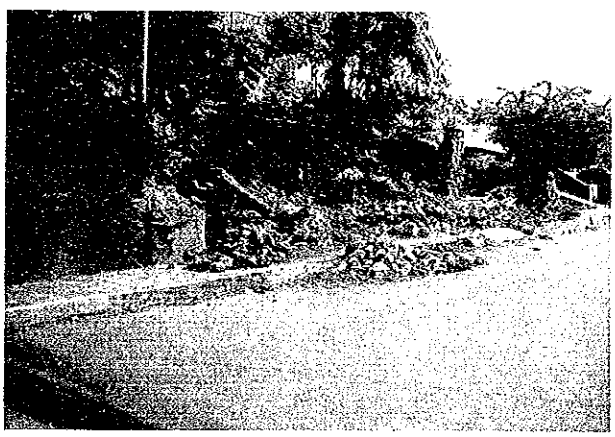

Photo 4.6 Collapse Example of Retaining Wall, Ende City

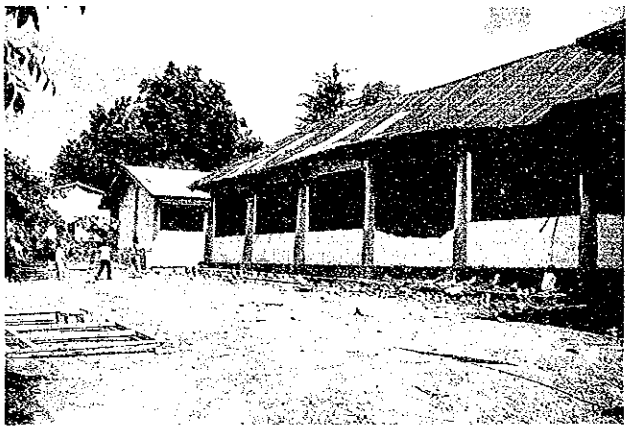

Photo 4.7 Severely Damaged Elementary School Building, Roof; Timber; Masonry, Column; Reinforce Concrete

Photo 4.8 Close Up of This School Building; Column Top and Ceiling

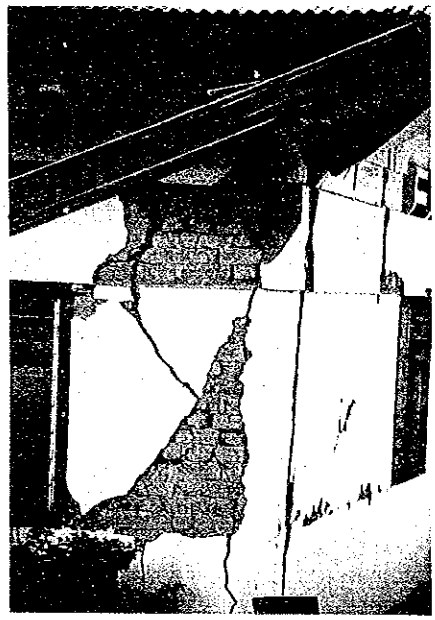

Photo 4.9 Adobe One Storey House, Severe Damage

Photo 4.10 Branch Office of Ministry of Public Works, Partially Collapsed

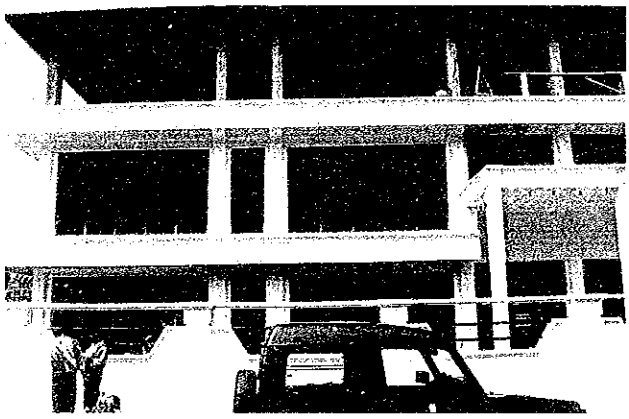

Photo 4.11 3-Storeyed Reinforced Concrete Building; Slight Damage, Under Construction

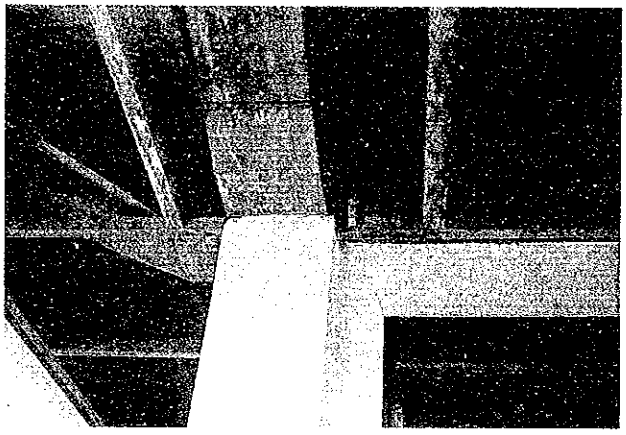

Photo 4.12 Same Building; Close Up of Beam-Column Joint at Top Floor

Photo 4.13 Example of Slight Damage of Masonry House

Photo 4.14 Medium Level Damage of Masonry Church

Photo 4.15 Collapse of Reinforced Concrete Building

Photo 4.16 3-Storeyed Reinforced Concrete Frame + Masonry Wall Building; Collapsed

Photo 4.17 Ende Assembly Hall; Collapse of Side Wall

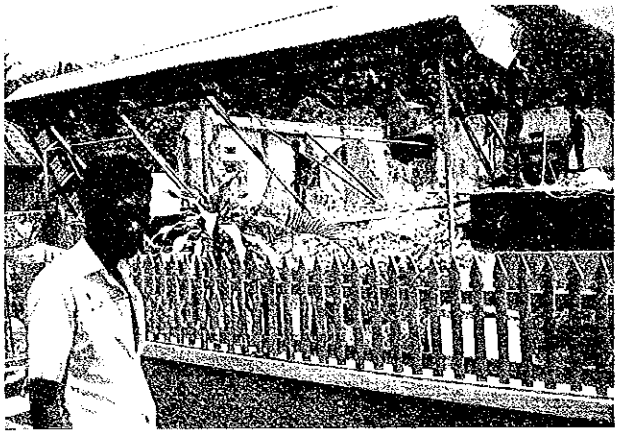

Photo 4.18 Typical Damage Pattern of Masonry Wall Building; Perfect Collapse

Photo 4.19 Typical Damage Pattern of Masonry Wall Building; Perfect Collapse

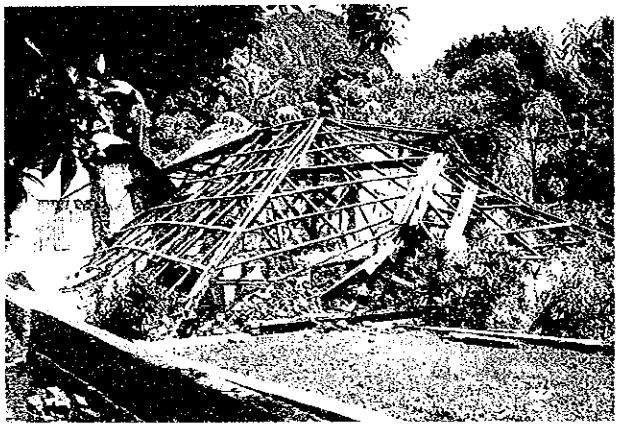

Photo 4.20 Collapse of Masonry House, Only Timber Roofing Frame Was Observed

Photo 4.21 Reinforced Concrete Tower Buiding; Slight Damage

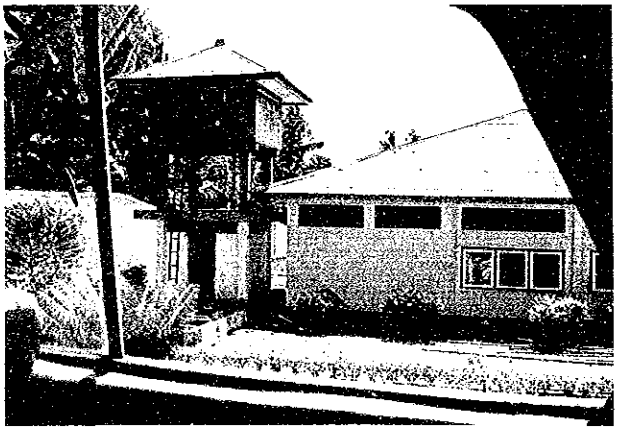

Photo 4.22 Same Type Reinforced Concrete Tower

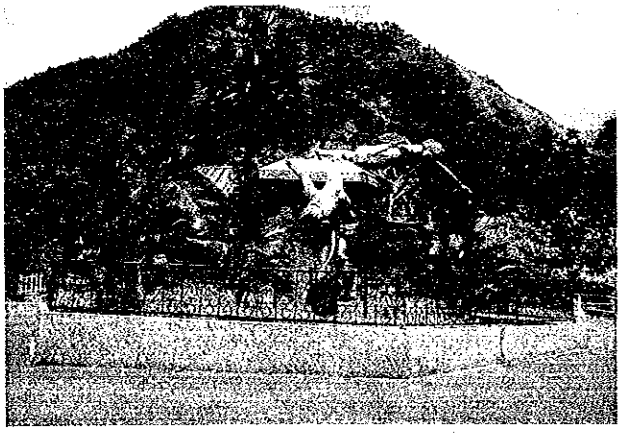

Photo 4.23 Reinforced (wire) Concrete Sculpture; Collapsed

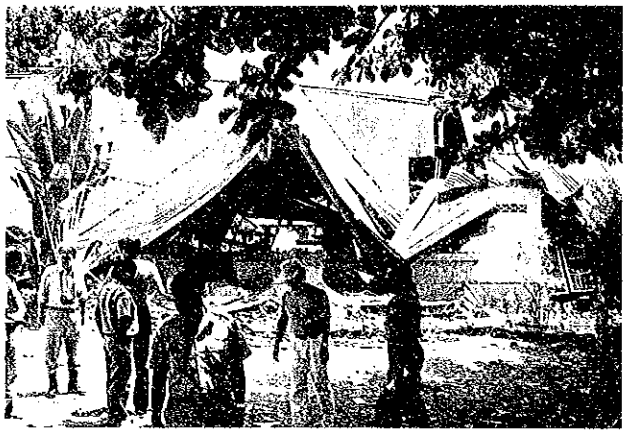

Photo 4.24 Religious House; Collapsed, Ende City

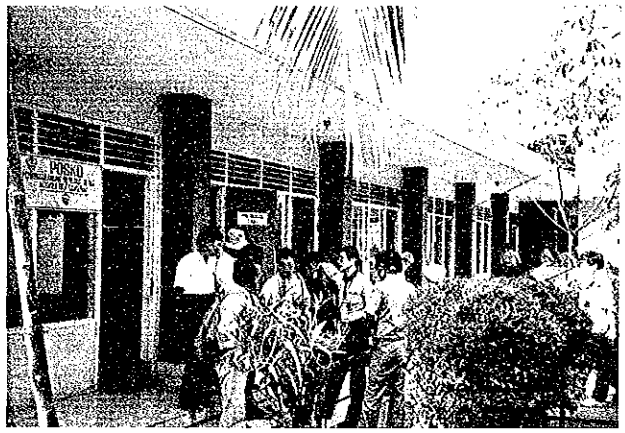

Photo 4.25 Base Camp Staff Official House; Reinforced Concrete

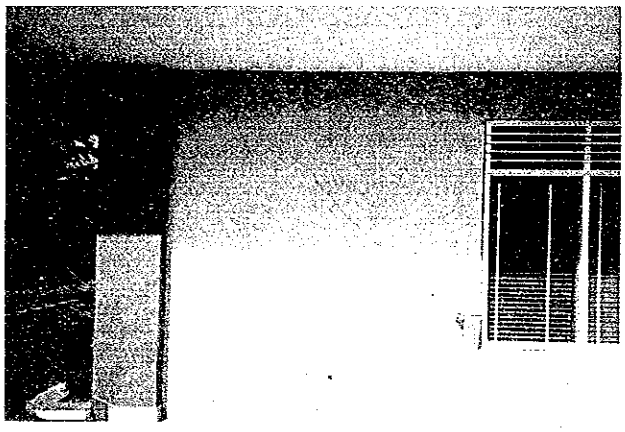

Photo 4.26 Same Building; Shear Diagonal Cracks are Observed

Photo 4.27 Collapsed House Due to Tsunami in Babi Island 30 km from Maumere City

Photo 4.28 Only Roofing of Mosque was Remaining in Babi Island

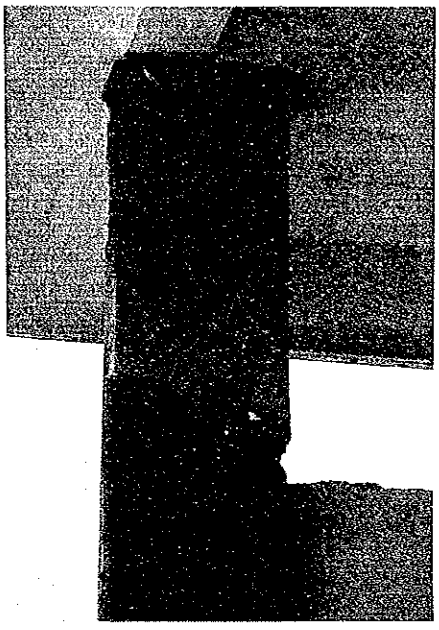

Photo 4.29 Airport Terminal Building (RC, one storey); Shear Failure Column Top

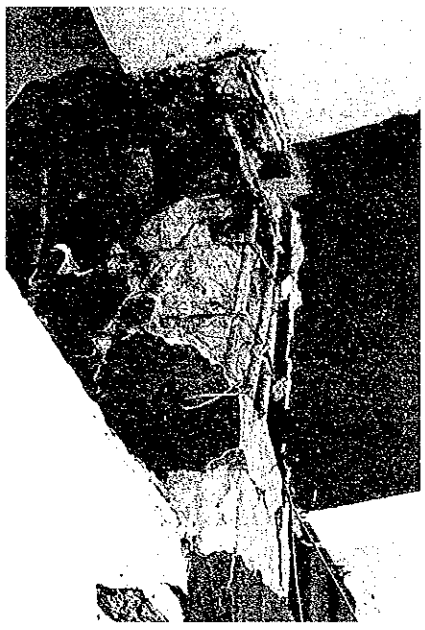

Photo 4.30 Airport Terminal Building (RC, one storey); Shear Failure Column Top

Photo 4.31 Superview of Babi Island

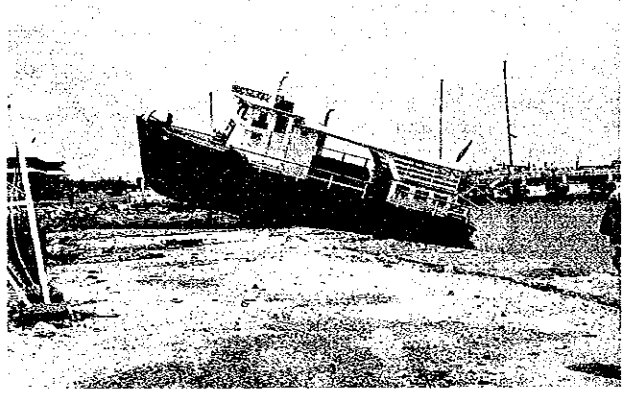

Photo 4.32 Damage of Maumere Port; Stranding of Steamer by Tsunami

Photo 4.33 Damage of Maumere Seaport by Tsunami

Photo 4.34 Perfect Colapse of Wulin Town by Tsunami 3 km West of Maumere

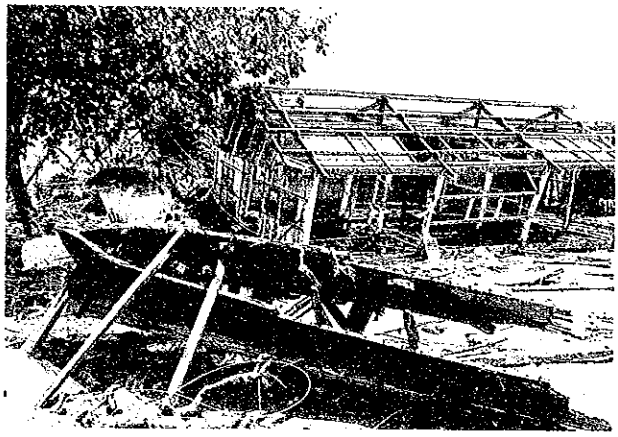

Photo 4.35 High Flooring Timber Houses Were Collapsed in Wulin; People Came from South Sulawesi Fishermen Race "Bugise"

Photo 4.36 Collapsed Masonry House in Maumere City

Photo 4.37 Slightly Damaged Masonry School Building in Maumere

Photo 4.38 Collapsed Mosque Along Sea Shore Street in Maumere City; Masonry Wall Structure, Timber Roofing

Photo 4.39 Severe Damage (out of plane break) of Wall System of Masonry Storage Building

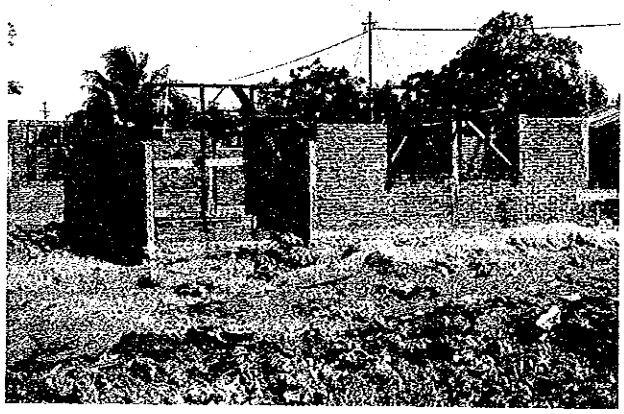

Photo 4.40 New Type Masonry Wall Building with Reinforced Concrete Framing; Under Construction

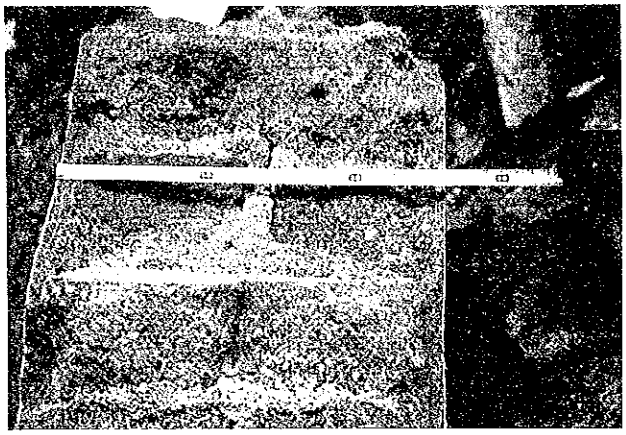

Photo 4.41 Cross Section of Masonry Wall from Collapsed Building

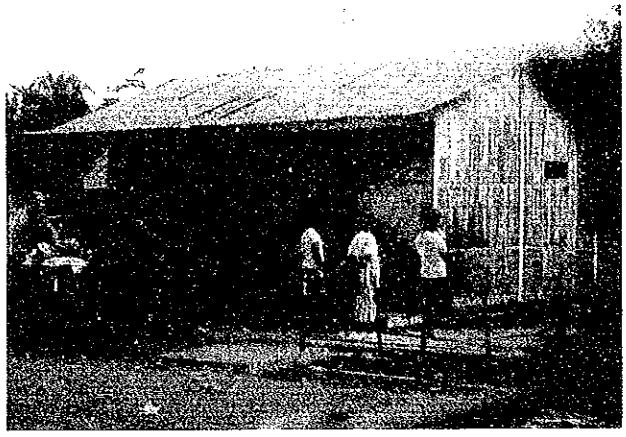

Photo 4.42 Timber and Bamboo House in Maumere City; No Damage, Timber Houses were Almost Non Damaged in Maumere City

Photo 4.43 Typical Collapse Pattern of Masonry House; Many of Masonry Houses were Collapsed Like This Pattern in Maumere City

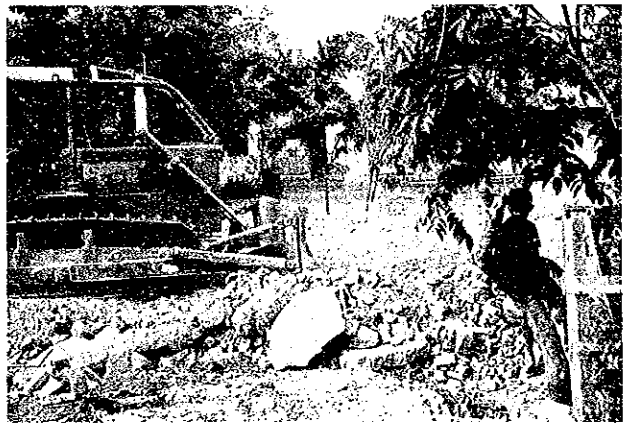

Photo 4.44 Military Staff Engaged in Demolishing and Recovery Works Two Weeks After the Earthquake, in Case of Masonry Structure, Demolishing is Easy

Photo 4.45 Two Storey Reinforced Concrete Masonry Building; Severe Damage, Business Work was Done in Temporary Facilitated Sheet Tent

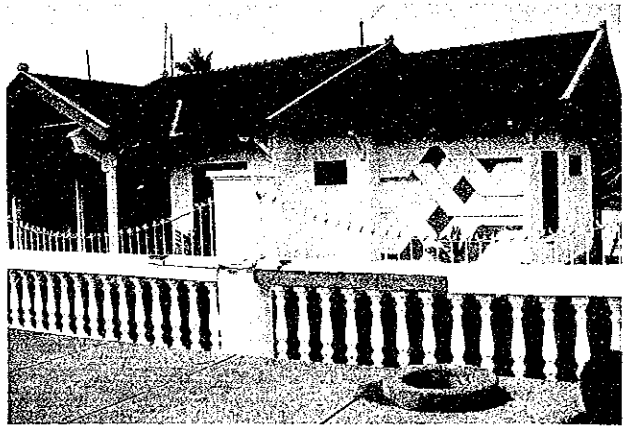

Photo 4.46 Well-Constructed Reinforced Concrete Masonry Wall Housing; Non Damaged, It Was Very Rare to See Non Damaged Such a Building

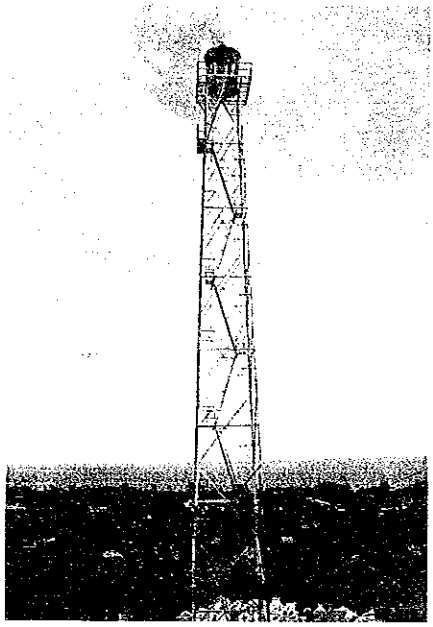

Photo 4.47 Steel Tower Locates in Southern Hill Side Area; Non Damaged

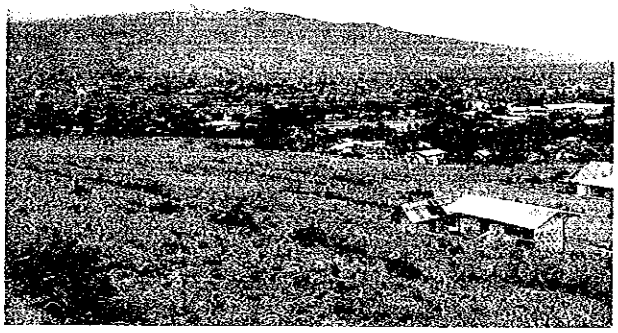

Photo 4.48-1 Total View of Maumere City; Wulin Town is Seen in Right Hand Side

Photo 4.48-2 Same as Left

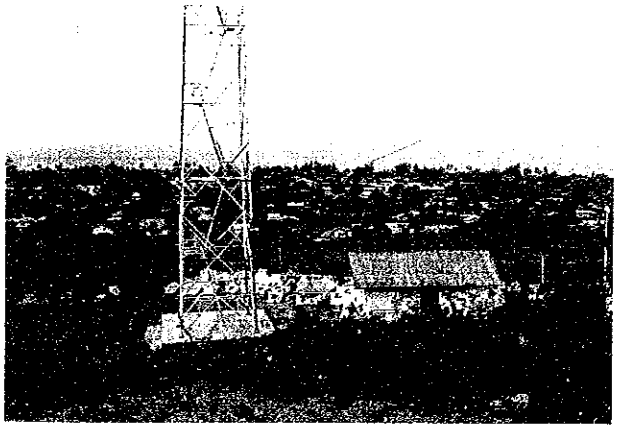

Photo 4.48-3 Maumere City; Babi Island is Seen Right Hand Side

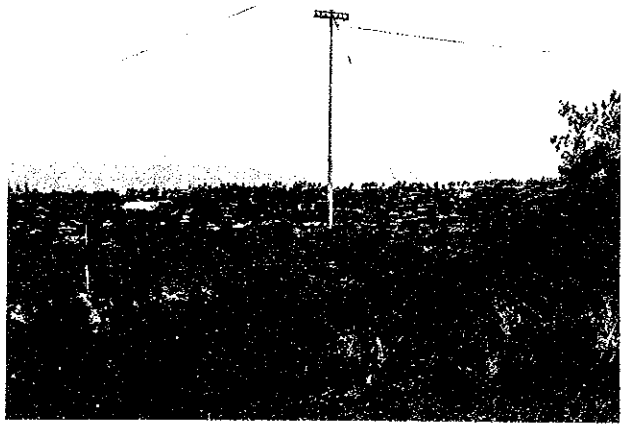

Photo 4.48-4 Same as Left

Photo 4.49-1 Refuge Tent Village in the Central Area of Maumere City

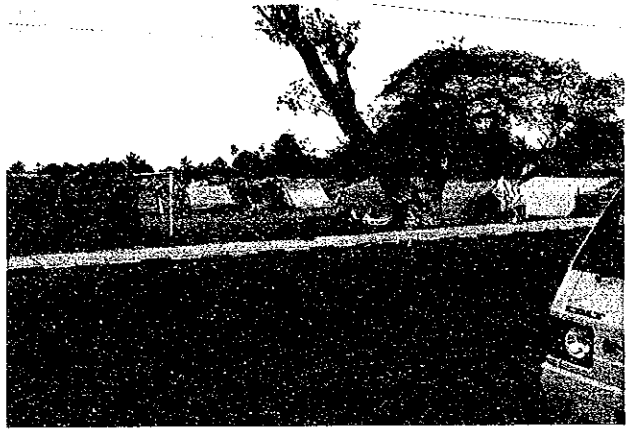

Photo 4.49-2 Same as Left

Photo 4.50-1 Severely Damaged Reinforced Concrete masonry Wall Building

Photo 4.50-2 Small Column and Small Size Reinforcing Bars of Same Buiding

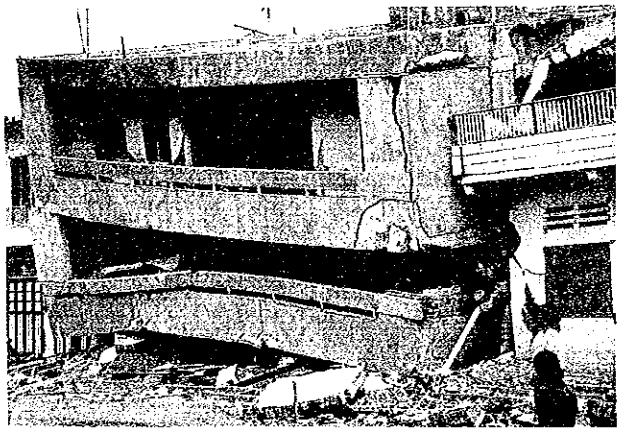

Photo 4.51-1 Collapse of Reinforced Concrete Building Which Seemed to be Heavier

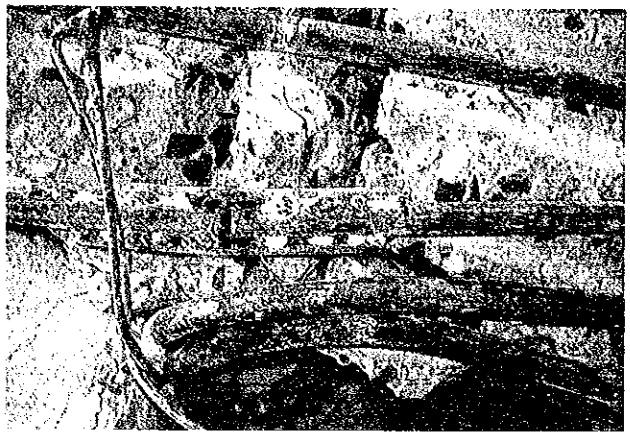

Photo 4.51-2 Close Up of This Building; Longitudinal Reinforcing Bars 29 mm Was Jointed by Welded Two 13 mm Bars

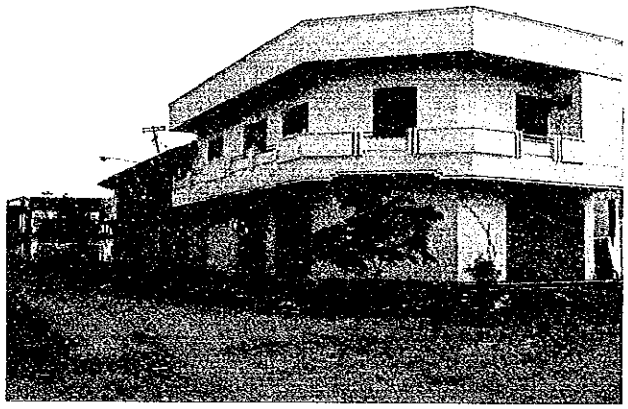

Photo 4.52 Reinforced Concrete Masonry Wall Building; Slight Damage Adjacent to the Building Photo No. 4.51

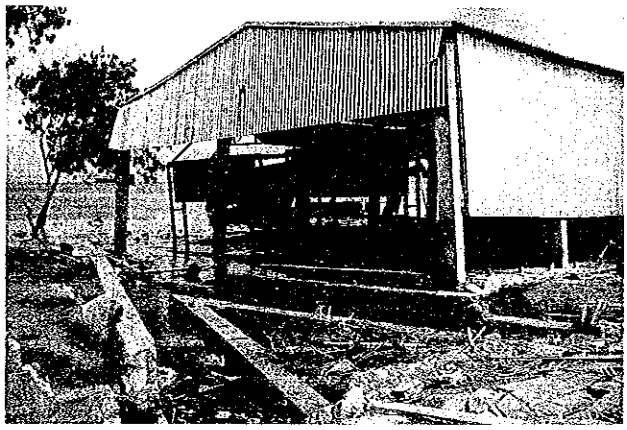

Photo 4.53 Freezing Factory of Fish Market; Damage of Settlement Due to Liquefaction

Photo 4.54-1 Damage of Road Observed in maumere City; Only This Area Was Damaged

Photo 4.54-2 Same as 4.54-1

Photo 4.55 Gasoline Stand Roofing at Hill Side Area of Maumere City; Steel, Non Damage

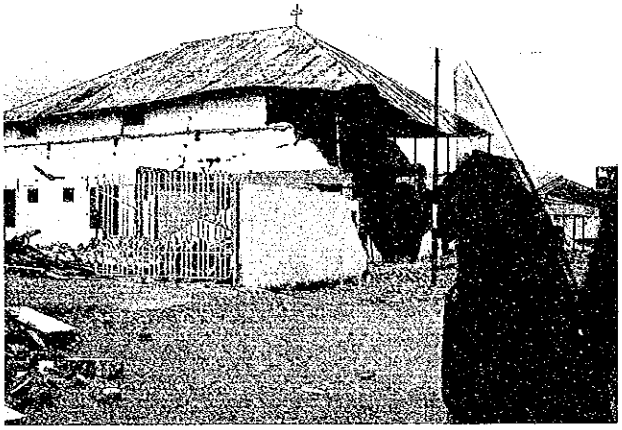

Photo 4.56 Out of Plane Collapse of Non Reinforcing Masonry Wall Structure

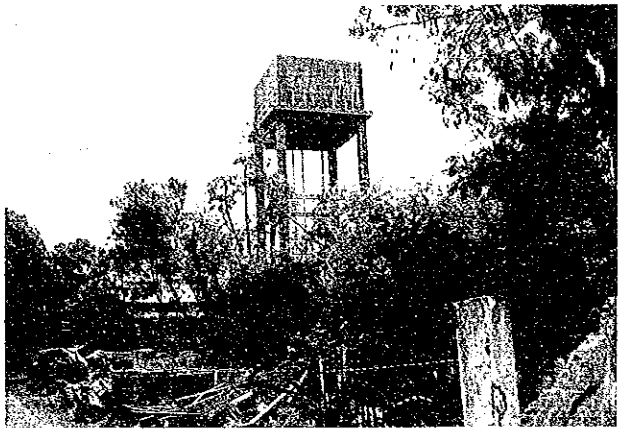

Photo 4.57-1 Reinforced Concrete Water Tank Structure; h=15 m; Slight Damage

Photo 4.57-2 Span: About 3 m, Column: 50 cm, Covering Mortar: 10 cm

Photo 4.58-1 Raw Material Clay of Red-Coloured Brick is Cut Off from Palm Tree Forests in Rainy Season (cross to Maumere City)

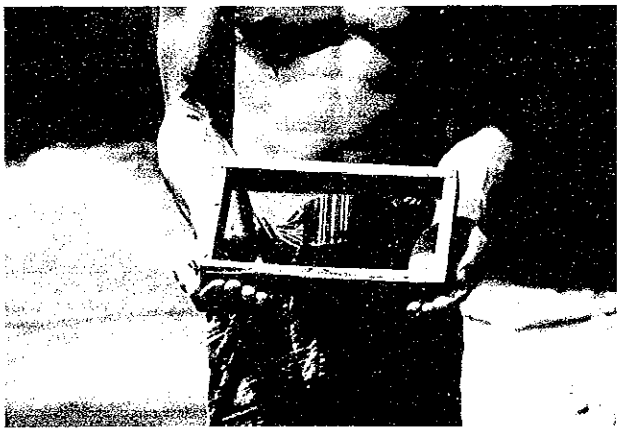

Photo 4.58-2 This Clay is Packed in the Wooden Frame, Size of Brick: 16×10×23 cm

Photo 4.58-3 Then This Raw Bricks are Burned for Twenty Four Hours; Combustion Material: Banana Trees

5. Damage of Lifeline Facilities

5.1 Introduction

Roads, bridges, ports, airports and utilities are the essential structures for life of people, and are therefore often referred to as the lifeline facilities. Features of the damage of lifeline facilities are described in this section.

5.2 Damage of Roads and Bridges

Extensive damage was developed in roads and bridges in Flores Island. Fig. 5.1 shows the major National Roads and Provincial Roads in the damaged area. Major damage was concentrated on the National Road connecting Ende and Maumere and Maumere and Larantuka, and the Provincial Road connecting Maumere and Magapanda. There are many other damages on local roads, but they could not be surveyed due to the limited schedule.

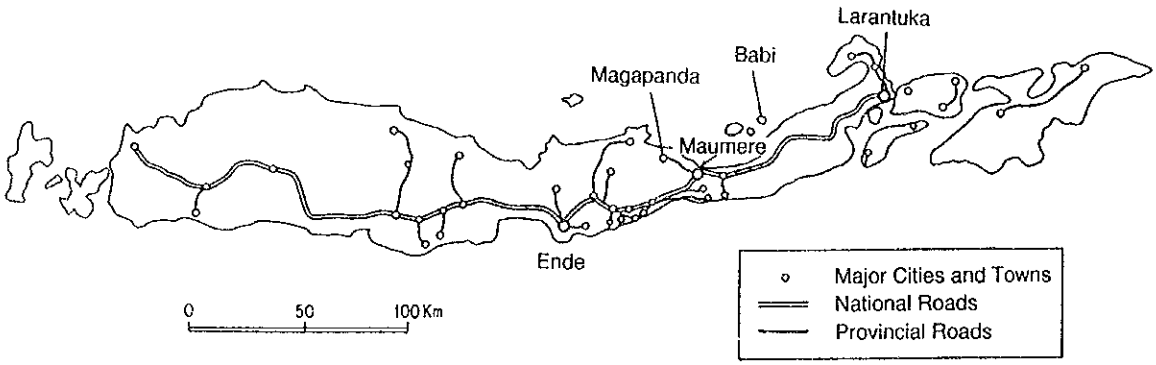

Fig. 5.1 Major National Roads and Provincial Roads in Flores Island

Feature of the damage depends on the soil and topographical condition at the site. Typical damages are as:

(1) National Road from Ende to Maumere

Figure 5.2 shows the major damage on the National Road from Ende to Maumere. Inspection was made for several kilometers from Ende and from Maumere to Lekebal. Although the damage was extensive at Ende side, it could not be inspected due to road damage. Because the road crosses the mountainous site, many slope failures were developed.

Because the surface at the site is deeply covered by soils, slope failure associated with soil mass was developed. Photo 5.1 shows a slope failure at road shoulder at the National Road several kilometers from Ende. The hill-side is of very steep rock. Photo 5.2 shows the slope failure on and under the Road. Photos 5.3 – 5.5 show the similar but more destructive slope failure. Rock fall was also observed, but it is not frequent between Maumere to Lekebal. They were weathered lime stone and sand stone.

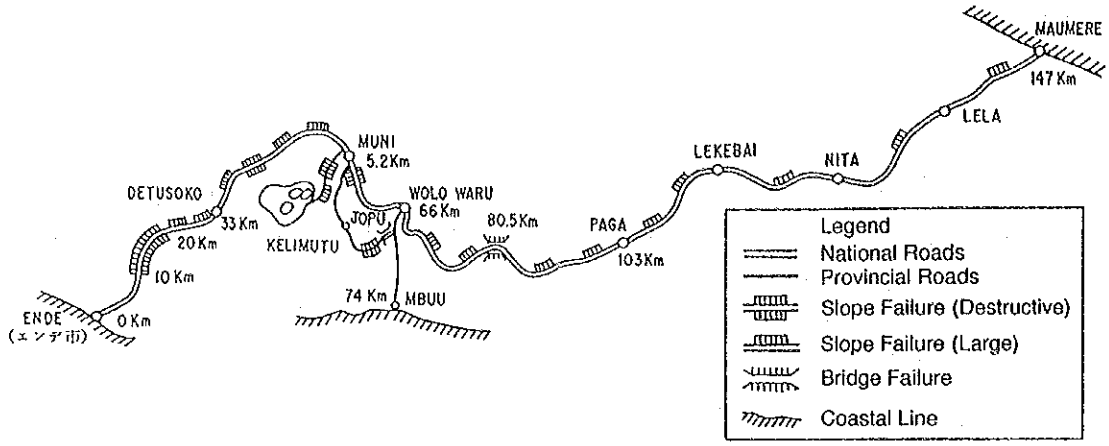

Fig. 5.2 Major Damage on National Road from Ende to Maumere

Figure 5.3 classifies the type of failures inspected. At the site where one side was cut and the other side was embanked (cut and filled embankment), the filled embankment often settled and this caused extensive cracks on the pavement as shown in Fig. 5.3(a) and (b). Failure also occurred at cut slope as shown in Fig. 5.3(c) and natural slope as shown in Fig. 5.3(d). The soil from the slope often suspended the road. This type of failure could be seen frequently. Destructive failure in which not only the cut slope but the natural slope failed as shown in Fig. 5.3(e) were also widely observed.

The slope failure was significant because the soils are of soft and wet clayey materials (volcanic ash). At the sites where scoria was observed as shown in Photos 5.6 and 5.7, the failure was induced at this layer.

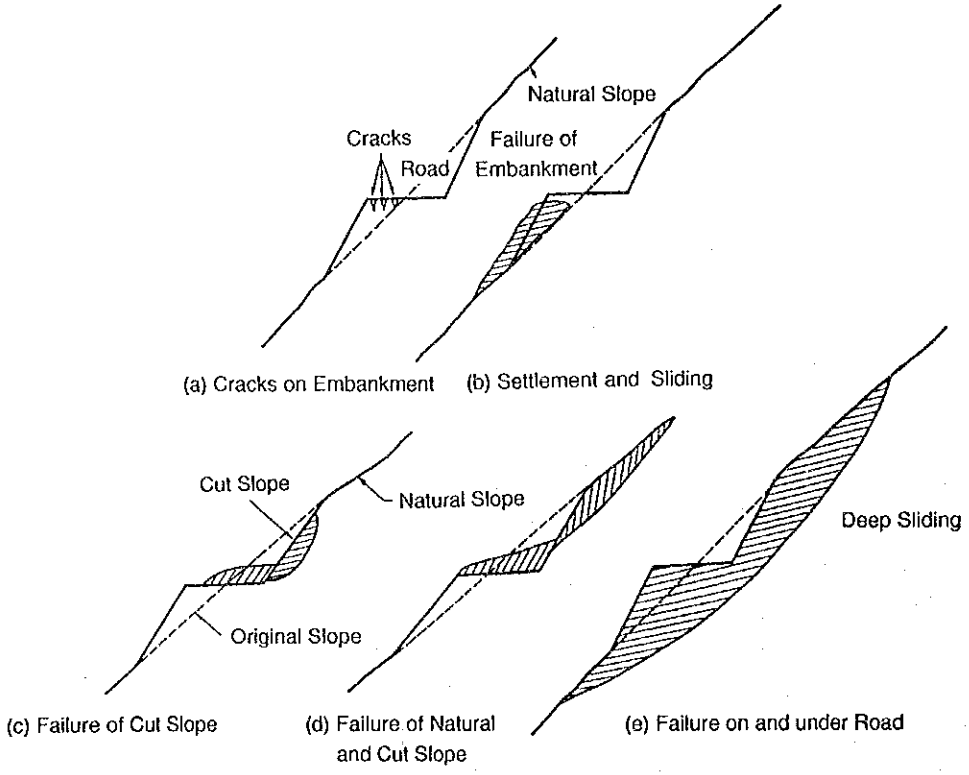

Fig. 5.3 Types of Slope Failure

(2) National Road from Maumere to Larantuka

Extensive damage of pavement and bridges were developed by soil instability. There are two types of bridges. One is the one-lane and small-span bridge. They are mostly single span or two span simply supported girder bridges. This type of bridges are very old, and were probably constructed before the Second World War. The second type of bridges is rather new. They are steel truss girders supported by reinforced concrete single columns or flame piers. Damage was mostly observed at the old bridges.

The most common type of failure was the settlement and tilting of abutments and back soils as shown in Photos 5.8 and 5.9. The settlement was as large as 1 m. It should be noted that such settlement and tilting of abutment were mostly caused by sliding of surrounding soils as shown in Fig. 5.4. Photo 5.10 shows large slidings developed near an abutment. Several sliding toward the center of a river was seen at this site. Photo 5.11 shows failure of soils in front of an abutment.

When only shallow soils slided, the abutments tend to tilt in the deck side, while when the sliding occurred deeply, the abutments tilted in back soil side. It is important to know that this is the damage caused by not vibration of the deck and abutment but the soil instability due to the earthquake. Therefore it is important to properly consider the large earth pressure due to such instability of surrounding subsoils into seismic design of bridges.

Contact of the abutments with the deck caused cracks at the abutments, because the deck resisted as the lateral beam between the two abutments. Some of them were extensively damaged as shown in Photo 5.12 and require full restoration.

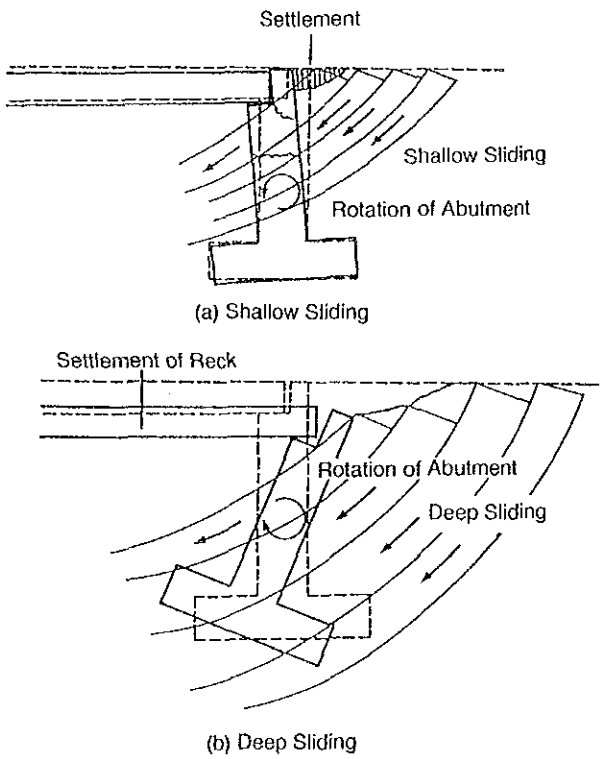

Fig. 5.4 Damage of Bridge Abutments due to Soil Instability

The seismic performance of new truss bridges as shown in Photo 5.13 performed basically well against the earthquake. The damage observed was the failure of anchor poles and cracks of parapet walls. The rubber cushion as shown in Photo 5.14 placed at the end of the deck behaved quite well for reducing the impact between the deck and the abutment wall. Although some of them suffered damage as shown in Photos 5.15 and 5.16, they can be easily repaired. At one bridge near Nebe, the lower chord (H-beam) at the first panel of the truss was buckled as shown in Photo 5.17 probably due to collision of the deck with the abutment.

The soil unsuitability caused the cracks on pavement as shown in Photo 5.18 at several sites. Depending on the size and degree of the soil sliding, the pavements suffered cracks in longitudinal (parallel to the road) and transverse direction.

(3) Provincial Road from Maumere to Magapanda

Along the Provincial Road from Maumere to Magapanda, there were several cracks and settlement of pavement associated with soil liquefaction. The largest settlement as shown in Photo 5.19 was developed at 15 km west of Maumere, and was as deep as 1 m. At this site, many sand valves associated with soil liquefaction were observed. The largest sand valve had the diameter of 2.1 m and the depth of 1.2 m as shown in Photo 5.20.

Photo 5.21 shows a large failure of abutments which simply support a deck. Large soil sliding as shown in Photo 5.22 was observed around the bridge.

Stone falling as shown in Photo 5.23 was observed near Magapanda.

5.3 Damage of Airports

The Control Tower of the Maumere Airport and the Ende Airport were badly damaged. The Control Tower at the Maumere Airport is four story masonry building, and was subjected to extensive shear failure at the wall with the glass being broken as shown in Photo 5.24. The control Tower at Ende Airport is three story masonry building, and was suffered significant shear failure at the wall as shown in Photo 5.25. The damage was so extensive that they could not be used. The apron and run-way suffer almost no damage at both Airports.

5.4 Damage of Ports

The Maumere Port as shown in Photo 5.26 suffered extensive damage due to soil liquefaction and tsunami in addition to the ground shaking effect. The quay wall and retaining wall for the apron overturned toward sea side and was badly damaged as shown in Photos 5.27 – 5.29. There were several ruptures on pavement at apron, as shown in Photos 5.30 and 5.31, which were developed due to soil liquefaction.

Soil liquefaction also caused extensive settlement and tilting at several buildings in the port as shown in Photos 5.32 and 5.33.

Photos 5.34 and 5.35 show a boat and a truck attacked by the tsunami.

5.5 Damage of River Hydraulic Structures

A water barrier on a river near Nebe suffered damage on the parapet wall of water gate as shown in Photos 5.36, 5.37 and 5.38. The parapet wall tilted with the back side being apart from the soil. Large settlement was developed at the back soils along the wall. Leakage of water from the parapet wall was seen. It is required to study the water path for preventing the possible increase of the leakage. Photos 5.39 and 5.40 show damage of water gate.

5.6 Damage of Utilities

Due to the limited time for survey, damage of electricity, telephone, water, sewer and gas could not be surveyed. The only information obtained during the survey is as;

At Ende, electricity is generated by 7 diesel engine generators as shown in Photo 5.41. They did not suffer damage. The building storing the generators suffered moderate damage; masonry wall fell down at two locations. Because cables distributing electricity were ruptured at several sites, the electricity was suspended after the earthquake. But it was rapidly repaired.

Water distribution was interrupted at wide area in Flores Island. The water was delivered by water-tank vehicles as shown in Photo 5.42.

5.7 Strong Ground Motion

Although it is said that 57 strong motion accelerographs are installed in Indonesia, no information regarding the location of the accelerographs and the strong motion records by the earthquake was obtained. Because the strong motion record is one of the most essential information for evaluating the intensity of ground shaking and structural response, it is advised to establish a system in which the information of strong motion records be available.

Because no measured information was available, the peak ground motion was estimated based on the Japanese empirical attenuation equation. Based on the statistical analysis of 394 components of strong motion record obtained at free field sites in Japan, the peak ground acceleration with the epicentral distance is given as[1];

$$a_{max} = 232.5 \times 10^{0.311M} \times (\Delta + 30)^{-1.218} \qquad (5\text{-}1)$$

where,

a_{max} : peak ground acceleration (cm/sec^2)
M : earthquake magnitude in Richter scale
Δ : epicentral distance (km)

Eqation (5-1) represents the peak ground acceleration at medium soil site.

It should be noted that Eq. (5-1) provides the mean value and that the scatter around the mean value is considerable. If one considers the deviation equivalent to one standard deviation from the mean value, the empirical estimation becomes either 1.7 times or 1/1.7 times of the mean value predicted by Eq. (5-1).

Assuming that the earthquake magnitude M of 7.5, the peak ground acceleration predicted by Eq. (5-1) attenuates as shown in Fig. 5.5. Because the epicenter of the earthquake was 8.48 S and 121.93 E, the epicentral distance at Maumere was about 50 km. It should be however noted here that because the fault zone is very close to the Flores Island, it is not appropriate to evaluate the distance from the epicenter. Assuming that the epicentral distance in Eq. (5-1) be measured from the center of the fault zone, the epicentral distance at Maumere and Ende is approximately 25 km and 80 km, respectively. The peak ground acceleration from Eq. (5-1) is therefore evaluated as 0.4 g at Maumere and 0.2 g at Ende. This value is considered to be a first-hand evaluation for the ground acceleration during the earthquake of December 12, 1992.

5.8 Soil Liquefaction

Soil liquefaction was developed extensively along the coast of Flores Sea. It is well known that the saturated alluvial sandy layer which has the water table within 10 m from the ground surface and has the D_{50}-value on the grain size accumulation curve between 0.02 and 2.0 mm are vulnerable to liquefaction[2].

Figure 5.6 shows a soil profile at Maumere. The ground condition is of sandy soils with the thickness of about 30 m – 50 m overlaid by the top soil with the thickness of about 5 m. Because water table is very high, the sand at Maumere is quite vulnerable to liquefacion.

Figure 5.7 shows the grain size accumulation curve for the three specimens obtained at three sites along the Flores Sea. The D_{50}-value is from 0.15 mm to 0.44 mm.

It is also known that the area in which liquefaction is induced increases as the earthquake magnitude increases. This relation is empirically obtained as[3]

$$\log \Delta = 0.77\ M - 3.6 \qquad (5\text{-}2)$$

where,

M : earthquake magnitude in Richter scale
Δ : epicentral distance (km)

Figure 5.8 shows the empirical relation by Eq. (5.2). It is not surprising from the past experience to have the liquefaction within 150 km from the epicenter for the earthquake of December 12, 1992.

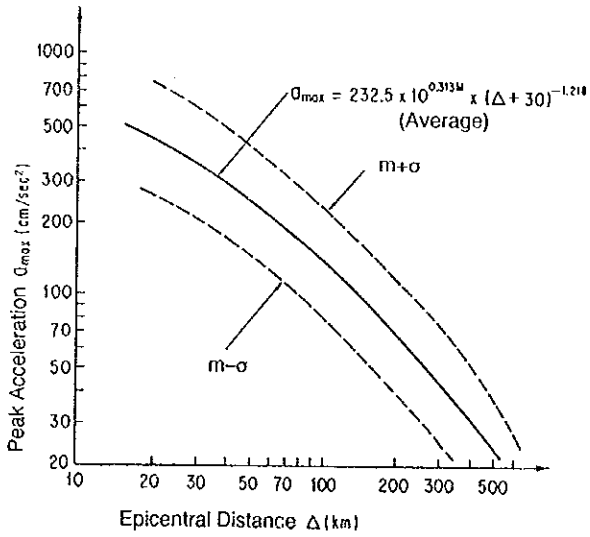

Fig. 5.5 Attenuation of Peak Ground Acceleration Estimated by Empirical Attenuation Equation

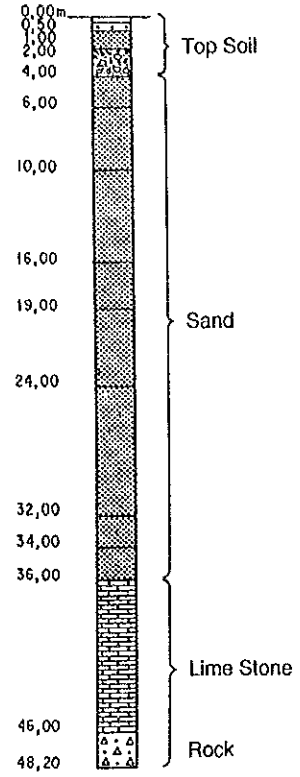

Fig. 5.6 **Soil Profile at Maumere City**

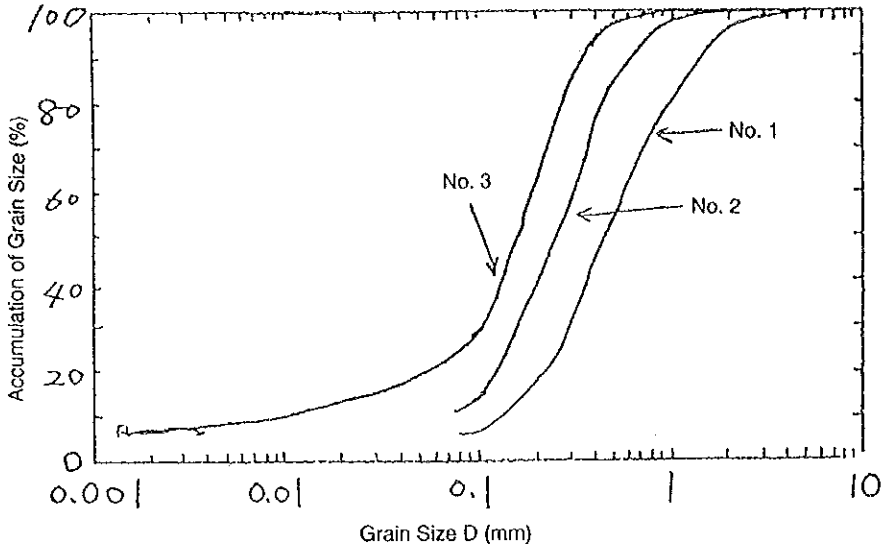

Fig. 5.7 **Grain Size Accumulation Curve of Sand**

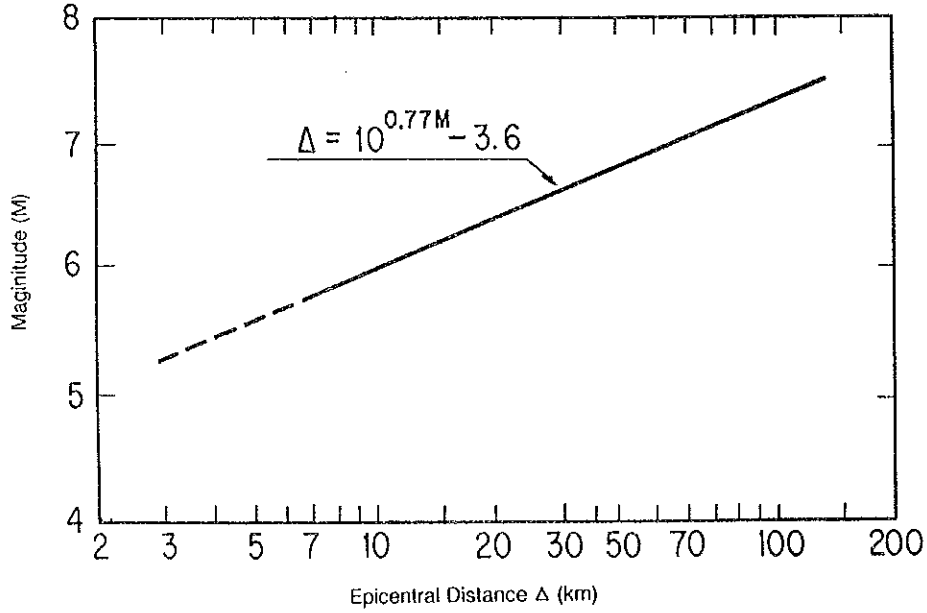

Fig. 5.8 **Empirical Distance from Epicenter in which Soil Liquefaction is Likely Developed**